Optical Technology for Microwave Applications II

Shi-Kay Yao
Chairman/Editor

Proceedings of SPIE—The International Society for Optical Engineering

Volume 545

Optical Technology for Microwave Applications II

Shi-Kay Yao
Chairman/Editor

April 9–10, 1985
Arlington, Virginia

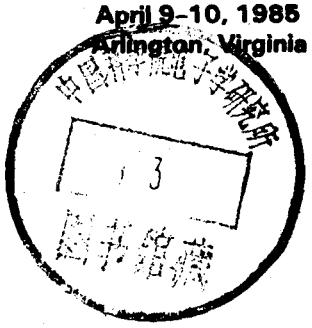

Published by
SPIE—The International Society for Optical Engineering
P.O. Box 10, Bellingham, Washington 98227-0010 USA
Telephone 206/676-3290 (Pacific Time) • Telex 46-7053

DR/6/28

The papers appearing in this book comprise the proceedings of the meeting mentioned on the cover and title page. They reflect the authors' opinions and are published as presented and without change, in the interests of timely dissemination. Their inclusion in this publication does not necessarily constitute endorsement by the editors or by SPIE.

Please use the following format to cite material from this book:
Author(s), "Title of Paper," *Optical Technology for Microwave Applications II,* Shi-Kay Yao, Editor, Proc. SPIE 545, page numbers (1985).

Library of Congress Catalog Card No. 85-061916
ISBN 0-89252-580-0

Printed in the United States of America.

OPTICAL TECHNOLOGY FOR MICROWAVE APPLICATIONS II

Volume 545

INTRODUCTION

This proceedings contains papers presented at the SPIE conference on Optical Technology for Microwave Applications II, held April 9-10, 1985 in Washington D.C. The meeting was devoted to the interdisciplinary area between the laser and electro-optics field and the microwave field. As the optical and electro-optical technologies advance in their signal carrying and signal processing capability, more applications are found in microwave signal transmission and in microwave signal processing. Yet the application of optical concepts to microwave devices and the interaction between optical radiation and microwave devices provide intriguing thoughts for the next generation of microwave systems. Some of these new technological thrusts are exhibited by this proceedings.

I wish to express my sincere appreciation to Harold R. Fetterman and John N. Lee for their efforts in helping me assemble this program. Their participation ensures a proper coverage of the various subjects in this interdisciplinary area and is the key to the success of this conference.

Shi-Kay Yao
TRE Semiconductor Equipment Corporation

OPTICAL TECHNOLOGY FOR MICROWAVE APPLICATIONS II

Volume 545

Conference Committee

Chairman
Shi-Kay Yao
TRE Semiconductor Equipment Corporation

Co-Chairmen
Harold R. Fetterman
University of California/Los Angeles

John N. Lee
U.S. Naval Research Laboratory

Session Chairmen
Session 1—Wideband Modulation and Transmission
Shi-Kay Yao, TRE Semiconductor Equipment Corporation

Session 2—Optics Applied to Microwave Devices
Harold R. Fetterman, University of California/Los Angeles

Session 3—Phase Array Applications
Shi-Kay Yao, TRE Semiconductor Equipment Corporation

Session 4—Optical Processor Components
John N. Lee, U.S. Naval Research Laboratory

Session 5—Acousto-Optical Processors
John N. Lee, U.S. Naval Research Laboratory

OPTICAL TECHNOLOGY FOR MICROWAVE APPLICATIONS II

Volume 545

Contents

OPTICAL TECHNOLOGY FOR MICROWAVE APPLICATIONS II

Volume 545

Session 1

Wideband Modulation and Transmission

Chairman
Shi-Kay Yao
TRE Semiconductor Equipment Corporation

High-Speed Optical Modulation Techniques

H.W. Yen, C.M. Gee and H. Blauvelt†

Hughes Research Laboratories
3011 Malibu Canyon Road, Malibu, Ca 90265

Abstract

In this paper, transmitter and receiver components for microwave fiber optic links are reviewed. Present link signal to noise limitations imposed by the performance of these components are analyzed, and promising trends in component development are discussed.

Introduction

Microwave fiber optic links consisting of a microwave modulated optical source, an optical fiber cable, and a high speed optical detector offer several advantages over coaxial links for rf transmission. These include low cost, low attenuation, light weight, immunity from electromagnetic interference, large bandwidths, and new signal processing capabilities.

In this paper, the characteristics of the various components of microwave fiber optic links at 0.83 μm and the impact of these characteristics on the overall link performance will be discussed. The primary emphasis of this discussion will be on the choice of components for optimizing the link signal to noise ratio.

Selection of Transmitter Components

Two approaches to modulating a semiconductor laser at microwave frequencies include direct modulation of the laser current and external modulation using electro-optic modulators. The performance of microwave fiber optic links will vary greatly depending upon which type of laser is used. For links using direct current modulation, the two most relevant laser diode operating characteristics are the modulation response and the intrinsic laser noise spectrum.

The frequency response of a laser diode under direct current modulation is influenced by both the intrinsic response of the laser and parasitic circuit elements associated with the laser packaging. The intrinsic small signal modulation response of a semiconductor laser is of the form:

$$S_{21} = \frac{1}{(f_r^2 - f^2)^2 + \gamma^2 f^2} \tag{1}$$

where f_r is the relaxation resonance frequency, a convenient measure of the useful bandwidth of a semiconductor laser. For most AlGaAs laser diodes, f_r is in the range 3-4 GHz at the maximum laser output power. However, by designing lasers to operate at higher output power densities or by decreasing the cavity lifetime, the resonance frequency can be increased. If laser diodes are designed in such a way as to minimize the effects of parasitic circuit elements then their frequency response is nearly the same as their intrinsic frequency response.

The second important operating characteristic of laser diodes for use in microwave fiber optic links is the intrinsic intensity noise spectrum of the laser. The intensity fluctuations of laser diodes arise from the shot noise processes associated with carrier injection and recombination inside the laser active layer.[1] These noise generating processes result in an intensity noise spectrum which is characterized by a broad and pronounced resonance at f_r. The laser fluctuations are expressed in terms of the relative intensity noise, RIN, defined as:

$$RIN(f) = \frac{\langle \Delta P^2(f) \rangle}{\bar{P}_L^2} \tag{2}$$

where P_L is the DC laser power and $\langle \Delta P^2(f) \rangle$ is the spectral density of the square of the laser optical power fluctuation.

The noise spectra of a Mitsubishi ML5101A "crank" TJS laser for various bias currents are shown in Figure 1. The most relevant feature of these curves is that the RIN below the

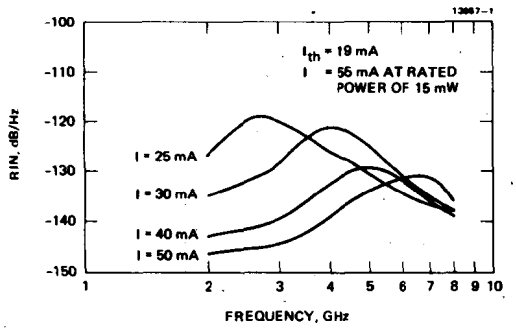

Figure 1. Relative intensity noise (RIN) of a Mitsubishi ML5101 laser.

resonance frequency f_r of 3-4 GHz decreases significantly as the bias current is increased. The noise spectra shown in Figure 1 represent the laser RIN under conditions of low optical feedback. In the presence of optical feedback levels as small as -60 dB, the intensity noise is increased. Low noise direct modulation fiber optic links must therefore either incorporate optical isolation, or new laser structures must be developed which are less sensitive to optical feedback.

Although external modulators have problems as well, external modulation links are not limited in frequency by the laser relaxation resonance. Perhaps even more important is the ability to use stable, low noise laser sources with external modulators. In this paper we will restrict our discussion to $LiNbO_3$ traveling$_2$wave Mach Zehnder modulator which has been demonstrated to have a 3 dB bandwidth[3] of 17 GHz.

The modulation transfer function for an interference type modulator, such as the Mach Zehnder modulator, is given by:

$$P = P_{pk} \sin^2\left(\frac{\pi V}{2V_\pi} + \Phi\right) \qquad (3)$$

where V_π is the "half-wave voltage", a parameter that takes into account the dimensions and material of the modulator. For linear modulation, the modulator is typically biased to $\Phi = \pm\pi/4$. The modulation characteristic is linear only for small signals around V=0, so distortion and the resulting intermodulation products will become an issue at high percentage modulation.

The capability of these modulators to operate at frequencies well above 10 GHz is a significant advantage of external modulation. The most serious disadvantage of using $LiNbO_3$ modulators in links operating at 0.83 μm is the limited optical power handling capability of the modulator. Due to photorefractive effects, less than 30 μW is typically launched into an optical fiber after taking into account propagation losses through the modulator and modulator-fiber coupling losses. Even for short links using efficient photodetectors, the DC photocurrent will be only of the order of 10 μA. As will be shown in the link analysis section of this paper, the receiver amplifier noise will be the dominant noise source in this case and the maximum S/N will be substantially less than that possible for links using direct current modulation at 0.8 μm wavelength.

Selection of Receiver Components

A receiver for a microwave fiber optic link consists of a high speed photodetector and a low noise amplifier. The detector should have a flat response over the frequency range of interest and as high an efficiency as possible. The amplifier should also have a flat response over the frequency range and as low a noise figure as possible.

At the Hughes Research Laboratories, GaAs Schottky photodiodes with bandwidths of 20 GHz and quantum efficiencies as high as 70% have been fabricated and characterized[3]. Based upon a 1.5 μm depletion layer width, the frequency limitation due to transit time effects is approximately 30 GHz. In normal operation with low input impedance amplifiers (eg. 50 Ω), the bandwidth is actually determined by the RC time constant of the device plus parasitic C and the amplifier input impedance, R.

Most links for transmitting analog microwave signals require bandwidths of a few GHz or less centered at the microwave carrier frequency. Detectors for microwave fiber optic links need to be designed so that the frequency response limited by transit time exceeds the carrier frequency, but the bandwidth limited by RC time constant need only exceed the link bandwidth. For most applications, the Schottky photodiodes described above will have bandwidths greatly in excess of that required when the detectors are operated into 50 Ω impedance amplifiers. The S/N of a receiver-amplifier-noise-limited link can be improved by increasing the amplifier input impedance, providing there is no corresponding increase in the amplifier noise figure. For links that are amplifier noise limited, it is therefore desirable to design amplifiers which have as large input impedances as possible, while still maintaining the $(RC)^{-1}$ bandwidth greater than the required link bandwidth. Tuned RLC circuits can be used to center the receiver bandwidth at the appropriate microwave carrier frequency.

Microwave Fiber Optic Link Analysis

In this subsection, we illustrate how the various parameters of a simple fiber optic link affect its signal-to-noise performance. Both direct laser current and external modulation techniques will be analyzed. The laser is characterized by a threshold current, I_{TH}; a maximum operating current I_{pk} (determined by signal distortion, or ultimately, by laser burnout); a slope efficiency, η_L [optical power/electrical current, $^{o}W/A$]; and an incremental drive impedance about its point of bias of R_L ohms.

The optical fiber is characterized by its power attenuation, K_F [$^{o}W/^{o}W$], which includes the optical coupling losses to both the laser and photodiode. The photodetector is characterized by a slope efficiency of η_D [$A/^{o}W$]. Photodiodes are usually characterized electrically as a current generator in parallel with a capacitance, C_D (the capacitance of the PN junction plus the lead and package parasitic capacitance). The proper terminating load should be chosen so that $(R_D C_D)^{-1}$ is large enough to pass the bandwidth, B.

We could define a current transfer function from laser to photodiode, $H_L' = \eta_L K_F \eta_D$. In terms of power rather than current, we introduce laser and detector transfer functions,

$$K_L = \eta_L / \sqrt{R_L} \tag{4}$$

$$K_D = \eta_D \sqrt{R_D} \tag{5}$$

We can now define an overall link transfer function,

$$H_L = K_L K_F K_D \tag{6}$$

which is dimensionless. The quantity H_L^2 is simply the electrical power transfer [$^{e}W/^{e}W$] between input and output of the link. It will generally be less than unity and therefore a loss rather than a gain.

We wish to find expressions for the signal-to-noise ratio of this link, and ultimately its noise figure in terms of the component parameters and system requirements. The equivalent electrical noise power generated in the laser is

$$N_L(f) = N_L'(f) - kTB = RIN_{DM}(f)(I_{BIAS}-I_{TH})^2 R_L B - kTB \tag{7}$$

where kTB is the thermal noise from the signal source impedance. RIN as defined in Eq (2) represents the total output noise from a laser as determined by measurement, including the thermal noise from the signal source, the shot noise associated with the DC laser current, and all other noise processes in the laser.

The photodetector output noise power, N_D, is the shot noise associated with the average photocurrent, I_D:

$$N_D = 2e\bar{I}_D F_D B R_D \tag{8}$$

where a factor $F_D \geq 1$ has been added to accomodate excess noise in the case of avalanche photodiodes. In terms of the laser current,

$$N_D = 2e(I_{BIAS} - I_{TH}) H_L F_D B \sqrt{R_L R_D} \tag{9}$$

The total noise power at the output of the link will then be the sum of the internal noise sources and the input noise, N_{in}=kTB, all referred to the output terminals.

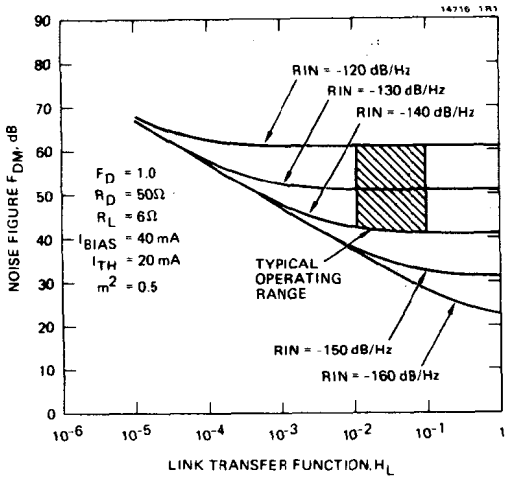

Figure 2. Noise figure attributable to the optoelectronic (laser, fiber, photodetector components of a direct modulation microwave link.

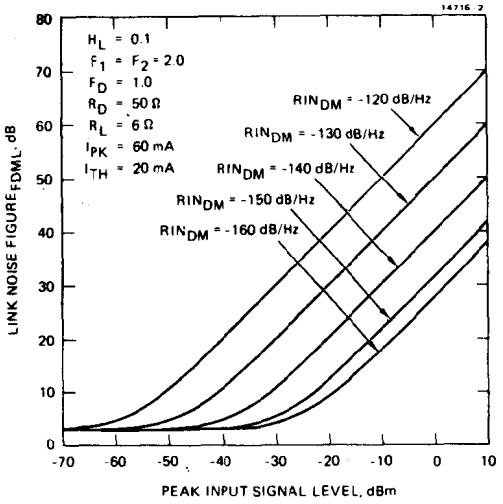

Figure 3. Overall link noise figure of a direct modulation microwave link.

$$N_{out} = H_L^2 N_{in} + H_L^2 N_L + N_D$$

$$= H_L^2 kTB + H_L^2[RIN_{DM}(I_{BIAS} - I_{TH})^2 R_L B - kTB] + 2e(I_{BIAS} - I_{TH}) H_L F_D B\sqrt{R_L R_D} \qquad (10)$$

so that the noise figure of this directly modulated link is :

$$F_{DM} = \frac{(S/N)_{in}}{(S/N)_{out}} = \frac{RIN_{DM}(I_{BIAS} - I_{TH})^2 R_L}{kT} + \frac{2e(I_{BIAS} - I_{TH}) F_D \sqrt{R_L R_D}}{H_L kT} \qquad (11)$$

F_{DM} is the noise figure that can be attributed to the optoelectronic components in the link (laser, fiber, photodetector). This noise figure is plotted in Figure 2 versus link transfer function H_L for different values of laser RIN. The values of the other relevant parameters are typical for direct modulation links using Mitsubishi ML5101 lasers. One of the most relevant features of this figure is that the noise figure attributable to the optoelectronic components is very large. The shaded portion of Figure 2 represents the range in which direct modulation links commonly operate. The dominant noise source in such links is laser noise. The noise figure is directly proportional to laser RIN and relatively insensitive to the link transfer function.

If we use amplifiers with noise figures $F_1, F_2 < F_{DM}$ before and after the link, respectively, we can generally improve the overall link noise figure. The overall link noise figure, F_{DML}, including the electronic amplifiers, may be determined from the noise figure cascade formula of Friis[4]:

$$F_{DML} = 1 + (F_1 - 1) + \frac{(F_{DM} - 1)}{G_{1DM}} + \frac{(F_2 - 1)}{G_{1DM} H_L^2} \quad . \qquad (12)$$

We see that to minimize the overall noise figure, we should maximize H_L. We would also like to choose the bias current so that the amplifier gain G_{1DM} is maximized (subject to the constraints of laser burnout and negative peak clipping) and RIN_{DM} is minimized. Taking $I_{BIAS} = (I_{TH} + I_{pk})/2$ then we would select:

$$G_{1DM} = (m^2/8S_{inpk})(I_{pk} - I_{TH})^2 R_L \qquad (13)$$

where m is the modulation depth and S_{inpk} is the peak rf power from the signal source (before the amplifiers). Then, we have the following expression for F_{DML}:

$$F_{DML} = F_1 - \frac{8S_{inpk}}{m^2(I_{pk}-I_{TH})^2R_L} + \frac{2S_{inpk}RIN_{DM}}{m^2kT} + \frac{8e\sqrt{R_D/R_L}S_{inpk}F_D}{m^2H_LkT(I_{pk}-I_{TH})} + \frac{8S_{inpk}(F_2-1)}{m^2H_L^2(I_{pk}-I_{TH})^2R_L} \quad (14)$$

The direct modulation link noise figure is shown in Figure 3. These curves show that when large input signal levels must be accomodated, the fiber optic link will seriously degrade the S/N. However, for low input signal levels the link noise figure is given by the preamplifier noise figure, F_1. The importance of using lasers with low RIN is also clearly indicated by Figure 3.

There are important differences between direct and external optical modulation which influence the performance of microwave fiber optic links. We will now derive expressions which describe the performance of a link incorporating a Mach-Zehnder interferometer modulator. The extension of these results to other types of external modulators follows accordingly.

The transfer function of Eq (3) can be expressed in terms of the rms signal drive power $S = V^2/2R_M$, where R_M is the modulator matched impedance (commonly 50 Ω). The optical power out of the modulator is

$$P = P_{pk}\sin^2\left[\frac{\pi\sqrt{2R_MS}}{2V_\pi} + \frac{\pi}{4}\right] \quad [^oW] \quad (15)$$

where we now are able to bias the laser to its peak power P_{pk}. We define the modulator transfer function to be:

$$K_M = \frac{\partial P}{\partial\sqrt{S}}_{S=0} = \frac{\pi P_{pk}\sqrt{2R_M}}{2V_\pi} \quad [^oW/\sqrt{^eW}] \quad (16)$$

The fiber link transfer function then becomes

$$H_M = K_MK_FK_D \quad (17)$$

As before, H_M^2 is the overall electrical transfer function from modulator to detector. The optical path transfer factor K_F will generally be smaller when an external modulator is used because of the propagation loss (a few dB) and coupling losses in the modulator.

Although the electro-optic modulator is, itself, a noiseless device, it passes along the thermal noise from the input amplifier via the transfer function, K_M. The laser, though now unmodulated, still contributes noise, which, as before, may be expressed in terms of the laser RIN. Thus, analagous to Eq (10) we may write the total noise out of an external modulator link as

$$N_{out} = H_M^2N_{in} + H_C^2N_L' + N_D = H_M^2kTB + H_C^2RIN_{EOM}(I_{BIAS}-I_{TH})^2R_LB + 2e(I_{BIAS}-I_{TH})H_CF_DB\sqrt{R_LR_D} \quad (18)$$

where H_C is the electrical transmission ratio from the laser terminals to the detector terminals [$\sqrt{^eW}/\sqrt{^eW}$]. H_C will generally have a smaller value than H_L because of additional optical losses, α, in K_F, and the laser power must be attenuated by some factor $y<1$ from its peak value to prevent optical damage of the modulator. Thus $H_C = \alpha yH_L$. RIN_{EOM} reflects the fact that a generally lower noise laser may be employed than in the case of direct modulation, RIN_{DM}.

We may then write the noise figure for the electro-optic modulated link, F_{EOM}, analogously to Eq (11) for F_{DM} as

$$F_{EOM} = 1 + \frac{RIN_{EOM}(I_{BIAS}-I_{TH})^2R_L}{kT}\left[\frac{H_C^2}{H_M^2}\right] + \frac{2e(I_{BIAS}-I_{TH})F_D\sqrt{R_LR_D}}{H_LkT}\left[\frac{H_C^2}{H_M^2}\right]\left[\frac{H_L}{H_C}\right] \quad (19)$$

Just as in the case of direct modulation, an E-O modulated link will be preceded and followed by amplifiers of gains G_{1EOM}, G_{2EOM}, respectively. In the case of an E-O modulated link, the constraint on G_{1EOM} is due to the modulator distortion at large modulation depths, m. The optical modulation depth for an E-O modulator for small modulation depths is given by

$$m = \frac{\pi V_{max}}{V_\pi} \quad (20)$$

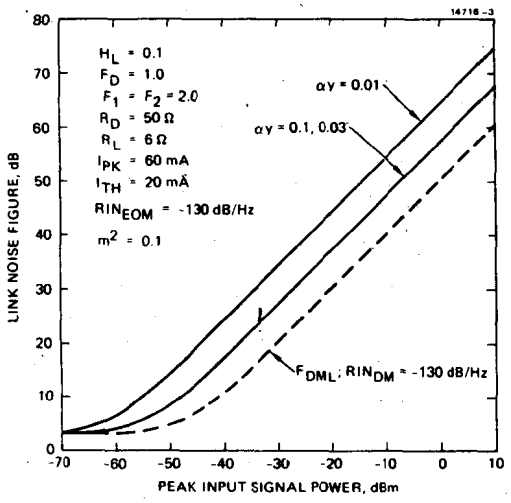

Figure 4. Overall link noise figure of an external modulation link incorporating a large RIN laser diode.

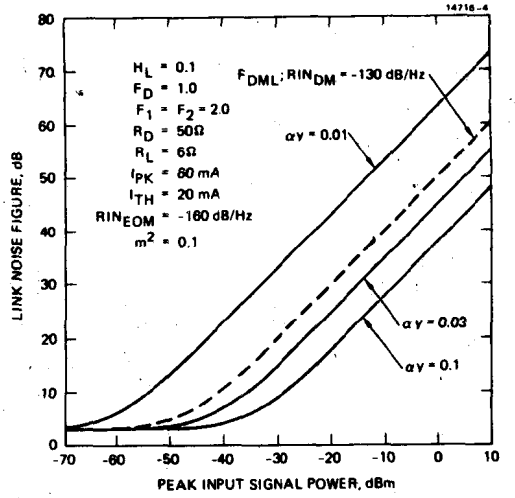

Figure 5. Overall link noise figure of an external modulation link incorporation a low RIN laser diode.

The constraint on G_{1EOM} can then be expressed as

$$G_{1EOM}S_{inpk} \leq \frac{m^2}{\pi^2}\left[\frac{V_\pi^2}{2R_M}\right] = \frac{m^2}{2}(I_{pk} - I_{TH})^2 R_L \left[\frac{H_C}{H_M}\right]^2 \qquad (21)$$

The overall link noise figure is then:

$$F_{EOML} = F_1 + \frac{2RIN_{EOM}S_{inpk}}{m^2 kT} + \frac{4eS_{inpk}\sqrt{R_D/R_L}\,F_D}{\alpha y m^2 H_L (I_{pk} - I_{TH})kT} + \frac{2(F_2 - 1)S_{inpk}}{\alpha^2 y^2 m^2 H_L^2 (I_{pk} - I_{TH})^2 R_L} \qquad (22)$$

The comparison between F_{DML} and F_{EOML} is illustrated in Figures 4 and 5. In both figures we assume RIN_{DM} = -130 dB/Hz and m=0.3. In Figure 4, we also take RIN_{EOM} to be -130 dB/Hz and plot F_{DML} and F_{EOML} for various values of αy. This corresponds to the situation where we are using the same laser for both the direct and external modulation links. Direct modulation is clearly superior. In Figure 5, we take RIN_{EOM} to be -160 dB/Hz. This corresponds to the case where a low noise, low bandwidth laser is used in the external modulation link. For small αy, direct modulation is still superior, but for $\alpha y \sim 1$, F_{EOML} can be significantly smaller than F_{DML}.

To summarize the most significant properties of direct and external modulation links:

- The contribution to the link noise figure from the post amplifier and detector shot noise are always larger in an external modulation link. This is due to the lower linear modulation depth, m, and the additional optical losses, α and y. With presently available $LiNbO_3$ guided wave modulators, these are the dominant noise sources of the external modulation links.

- If identical lasers and bias currents are used in direct modulation and external modulation links, then the laser noise contribution to the link noise figure will be larger in the external modulation link, due to the lower linear modulation depth.

- Direct modulation links operate at $f \leq f_r$ where laser RIN is large. Laser noise is the dominant noise source in low optical loss direct modulation links.

- External modulation links can use lasers with $f_r \ll f$. In this case the laser noise contribution to the link noise figure can be negligibly small. If the optical losses in the external modulation link are also small, then the external modulation link noise figure can be lower than that of a direct modulation link.

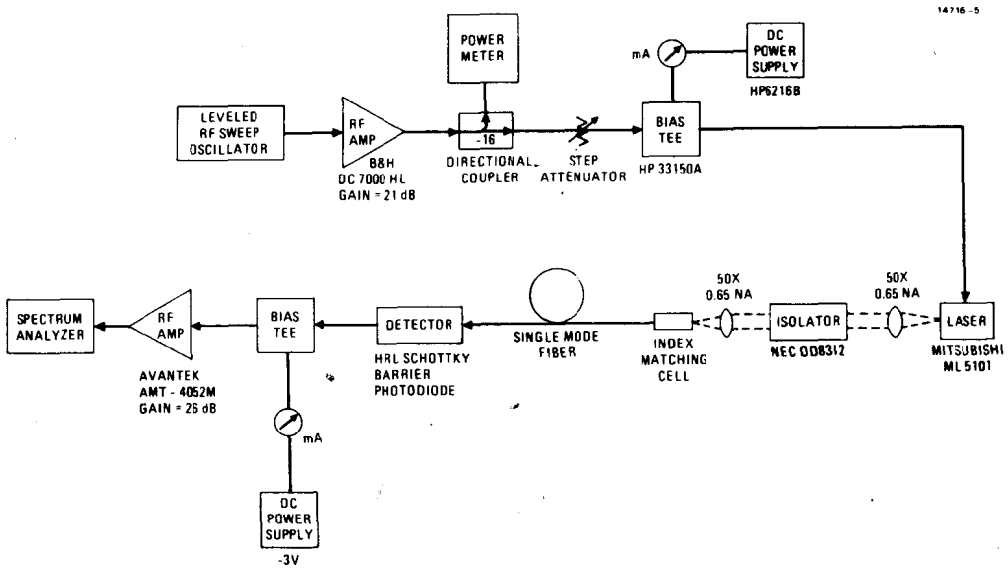

Figure 6. Experimental arrangement for evaluating the performance of microwave fiber-optic links.

Microwave Fiber Optic Link Performance

In the preceeding sections, the characteristics of the transmitter and receiver components of a microwave fiber optic link and the impact of these characteristics on link performance have been discussed. In this section, the actual performance of a short link will be described.

The components used in an actual link are shown in Figure 6. This link has been characterized over the frequency range of 2-8 GHz. We found that the Mitsubishi ML 5101A laser resulted in the best link performance due to its low RIN and relatively flat frequency response in the 2-8 GHz frequency range. The optical isolator was included to minimize optical feedback into the laser diode. Optical feedback from the near end of the single mode fiber was found to greatly increase the laser noise when the isolator was omitted. The receiver for this link consisted of Schottky photodiodes fabricated at Hughes Research Labs[3] and commercially available GaAs amplifiers. The dominant noise source of this link was the laser diode noise. The fiber optic link had an rf power loss, H_L^2, of 33 dB at 3 GHz. The rf transfer function is given by:

$$H_L^2 = n_L^2 K_F^2 n_D^2 (R_D/R_L) \qquad (23)$$

Of this loss, 11 dB was attributable to the laser DC differential quantum efficiency of 28% per facet, 10 dB was due to the laser parasitics and packaging, which reduced the laser efficiency below the DC level, 12 dB was due to the optical coupling losses and fiber attenuation, and 9 dB was due to the detector quantum efficiency of 35%. 9 dB of signal gain could be attributed to the ratio of the detector to laser impedances (R_D = 50 Ω, R_L = 6 Ω). Although we do not believe that the rf link loss of 33 dB resulted in any significant degradation of the link performance (see Figure 2), the link loss can probably be reduced to less than 15 dB by eliminating the laser packaging rolloff, improving the laser-fiber coupling, and improving the detector quantum efficiency.

We have measured the link S/N of a link consisting of a directly modulated Mitsubshi ML5101A laser, a 250 m single mode fiber, a Hughes Schottky photodiode, and commercial GaAs amplifiers. The signal to noise per unit bandwidth that we were able to achieve is shown in Figure 7. Also shown in this figure is the expected link S/N assuming 70% depth of modulation. The discrepancy between the two curves is partially due to a lower depth of modulation in the actual links, particularly at the higher frequencies. We limited the rf input power in the link S/N measurements to 5 mW, because of concerns about the effect of large rf drive powers on the laser reliability. We also observed that the presence of the rf signal made the laser more sensitive to optical feedback. Particularly noticeable was an increase in the laser noise at frequencies near the modulation frequency, which degraded the

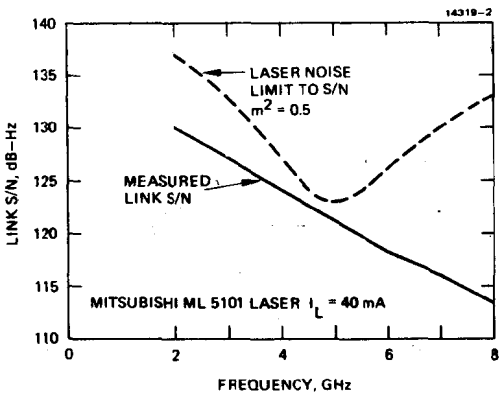

Figure 7. Experimentally observed link S/N for a direct modulation link.

link S/N by 2-5 dB. Eliminating the fiber did not significantly change the link S/N. However, care had to be taken to minimize optical feedback from the fiber ends.

This work has been funded in part by Solid State Sciences Division of the Rome Air Development Center.

References

† Present address: Ortel Corporation 2015 W. Chestnut St, Alhambra, CA 91803.

1. C. Harder, J. Katz, S. Margalit, J. Shacham, and A. Yariv "Noise Equivalent Circuit of a Semiconductor Laser Diode" IEEE J. Quant. Electron. QE-18 pp. 333-337 (1982).

2. C. Gee, G. Thurmond, and H. Yen "17 GHz Bandwidth Electro-optic Modulator Appl. Phys. Lett. 43 pp. 998-1000 (1983).

3. H. Blauvelt, G. Thurmond, J Parsons, D. Lewis, and H. Yen "Fabrication and Characterization of GaAs Schottky Barrier Photodetectors for Microwave Fiber Optic Links" Appl. Phys. Lett. 45 pp. 195-196 (1984).

4. H.F. Friis, Proc. IRE, 32 p419 (1944).

17 GHz Direct Modulation Bandwidth and Impedance Characteristics of Vapor Phase Regrown 1.3 μm InGaAsP Buried Heterostructure Lasers

C. B. Su, V. Lanzisera, W. Powazinik, E. Meland,
J. Schlafer, R. Olshansky, and R. B. Lauer

Optoelectronic Devices Department, GTE Laboratories Inc.,
40 Sylvan Road, Waltham, Massachusetts 02254

Abstract

A record room temperature small-signal modulation bandwidth of 17 GHz is reported for vapor phase regrown 1.3 μm InGaAsP buried heterostructure (BH) lasers operated at a pulse bias optical power of only 12 mW/facet. Under cw bias conditions a bandwidth of 12 GHz is achieved. The optical modulation amplitude remains flat in sharp contrast to other types of BH lasers which exhibit strong signal roll-off at frequencies well below the resonance frequency. The modulation bandwidth is attained by increasing the p-doping level in the active region and by the choice of short cavity length. The device is grown on a conductive substrate indicating that it is unnecessary to use a semi-insulating substrate to obtain flat optical response in these vapor phase regrown BH lasers.

Introduction

Very high frequency direct modulation bandwidth of AlGaAs and InGaAsP diode lasers have been reported[1-2]. An intrinsic modulation bandwidth of 12.5 GHz of 1.3 μm InGaAsP vapor phase regrown buried heterostructure lasers (VPR-BH) under pulse bias operation was previously demonstrated[2]. In this paper, a small signal modulation bandwidth of a record 17 GHz is reported for the VPR-BH lasers operated at a pulse bias optical power of only 12 mW/facet, and a bandwidth of 12 GHz is obtained for cw bias conditions. Impedance measurements were also performed on the VPR-BH lasers. The low parasitic capacitance ($\leq$ 2 pF) estimated from these measurements explains the observed absence of optical modulation roll-off.

According to a small-signal analysis,[3,4] the resonance frequency f_o can be written as:

$$f_o \propto \sqrt{(A/L)(\alpha_T/\alpha_m)P_b}, \qquad (1)$$

where P_b is the bias optical power, α_T is the total optical loss, α_m is the mirror loss, A is the differential gain constant, and L is the cavity length.

The use of a short cavity laser biased at high power is commonly employed to increase f_o (bandwidth). It has been reported that the differential gain constant A can be dramatically increased by increasing the active region p-doping level[5,6]. According to Eq. (1) the modulation bandwidth can thus be appreciably increased by increasing the active layer doping level. This new feature is used in this work to increase the bandwidth of VPR-BH lasers.

The devices used in these modulation experiments are similar in structure to BH lasers in which the lateral confining InP regions are obtained by the mass transport phenomena[7,8]. For the VPR-BH lasers the lateral confining InP regions are obtained by vapor phase regrowth rather than mass transport. For this wafer, the p-doping level in the active region is about 2×10^{18} cm^{-3}. The diode cavity length is 112 μm and the diode width is 250 μm. The top and bottom metallic surfaces are unetched. The room-temperature threshold current is 28 mA and the differential quantum efficiency is 40%. The diodes are mounted on a microstrip line such that the total package including the laser chip has an insertion loss of less than 1.5 dB to 20 GHz.

The block diagram of the experimental set-up is shown in Figure 1. The electrical and optical signals are displayed on sampling scopes with S-4 heads which also

function as 50Ω loads. A 20 GHz GTE InGaAs PIN diode is used for optical detection.

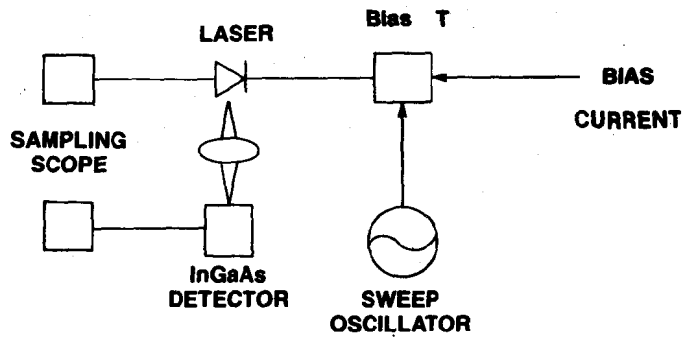

Figure 1: Block diagram of the experimental set-up

Modulation Bandwidth

In Figure 2, the optical response to a constant amplitude small signal sinusoidal driving current is shown at different frequencies and different bias optical power for the case of cw bias operation. A bandwidth of 12 GHz is achieved without a pre-resonance roll-off at a bias optical power of only 6.6 mW/facet. This is the highest bandwidth ever reported for InGaAsP lasers under cw operation. Under pulse bias operation at an optical power of 12 mW/facet, a bandwidth of 17 GHz is achieved as shown in Figure 3.

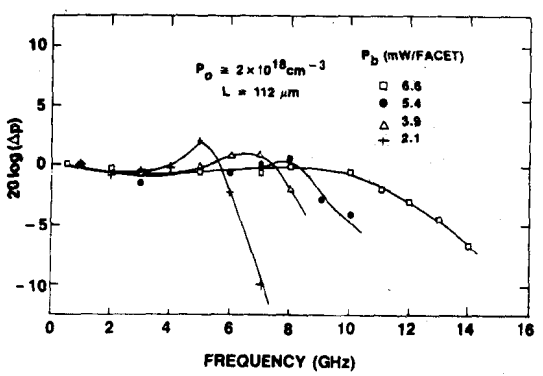

Figure 2: The normalized small signal optical response versus frequency under cw operation.